Pergamon

Int. J. Engng Sci. Vol. 36, No. 1, pp. 49–60, 1998

Printed in Great Britain
PII: S0020-7225(97)00058-X
0020-7225/98 $19.00 + 0.00

ANALYTICAL SOLUTIONS FOR FREE CONVECTION FLOW OF A PARTICULATE SUSPENSION PAST AN INFINITE VERTICAL SURFACE

ALI J. CHAMKHA* and HASSAN M. RAMADAN

Department of Mechanical and Industrial Engineering, Kuwait University, Safat, 13060 Kuwait

Abstract—Continuum equations governing steady, laminar, free convection flow of a particulate suspension past an infinite porous vertical flat plate are developed. These equations account for particulate viscous effects which are absent from most two-phase flow models. Analytical solutions for inviscid and viscous particle phase of uniform density distribution are obtained. Graphical results for velocity and temperature profiles of both phases based on the analytical solutions are presented and discussed. In addition, tabulated results for the skin-friction coefficients of both phases and the Nusselt number of the fluid phase are shown. A parametric study of some of the physical parameters involved in the problem is conducted to elucidate interesting features of the solutions. © 1997 Elsevier Science Ltd.

1. INTRODUCTION

Buoyancy-induced flow and heat transfer has attracted the interest of many investigators over the past two decades [1–6]. This interest stems from the possible applications of these studies in many industries. Examples of processes in these industries include geothermal reservoirs, petroleum reservoirs, chemical reactors, energy storage systems and many others. In spite of the high possibility of particulate entrainment into such flows, there has been no significant work in the open literature done on free convection flow and heat transfer for a dusty fluid. Analysis and study of free convection of a particulate suspension over surfaces or in enclosures requires the consideration of two-phase flow models. The two main modeling approaches for a particulate suspension available in the literature are the continuum approach in which both phases are treated as interacting continua (see, for instance, Marble [7] and Ishii [8]) and the lagrangian approach in which only the fluid phase is treated as a continuum and the particle phase is governed by the kinetic theory (see, for example, Berlemont *et al.* [9]). The equations governing a two-phase fluid-particle system are rather complex to preclude analytical solutions except in very idealized special cases. This paper considers free convection flow and heat transfer of a particulate suspension along a vertical infinite porous flat plate. The motivations for considering this problem are the apparent absence of a two-phase theory for buoyancy-induced flows and that it exhibits a boundary-layer type behaviour in which its governing equations reduce to ordinary differential equations which can be solved in closed form. The flow is assumed to be steady and laminar and the properties of both the fluid and the particle phases are assumed constant except for the fluid-phase density in the buoyancy term in the fluid-phase momentum equation. In reality the particle-phase density distribution is not uniform and all particles are not of one size, and is affected by the presence of the boundary layer. However, since a major objective of this work is to obtain closed-form solutions, the particle phase is assumed viscous, monodispersed, and its density is assumed to be uniform. It should be noted that if more than one-size particles are present in the suspension, then the problem becomes more involved as the number of phases increases. The concept of the particle-phase viscosity has been employed by many previous investigators (see, for instance, Gadiraju *et al.* [10], Gidaspow

* Corresponding author.

[11], and Tsuo and Gidaspow [12]). It can be used to represent Reynolds stresses arising from turbulent flows, particle-particle interaction in dense suspensions, and as a smoothing mechanism to facilitate numerical solutions. It can also be thought of as a natural consequence of the averaging processes normally employed to represent a discrete system of particles as a continuum (see, for example, Drew [13], and Drew and Segal [14]).

1.1 Governing equations

Consider steady laminar buoyancy-induced flow of a fluid–particle suspension along an infinite porous vertical flat plate. Let x be the distance along the plate and y be the distance normal to it. The plate is coincident with the plane $y=0$. The ambient fluid away from the plate surface is assumed stagnant and the particles are assumed free falling in the direction of gravity (see Fig. 1). Uniform fluid-phase suction with velocity V_w is imposed at the plate surface which is maintained at a constant temperature T_w. All properties of the suspension are assumed to be constant except the fluid density in the buoyancy term of the fluid-phase linear momentum equation. The governing equations for this investigation are based on the balance laws of mass, linear momentum, and energy for both the fluid and the particle phases. Since the plate is assumed infinite, the dependence of variables on the x direction will be negligible compared with that of the y direction. Therefore, all the dependent variables will only be functions of y. Under this and the previous assumptions, the governing equations are given by the following balance laws of mass, linear momentum, and energy

$$\frac{dv}{dy} = 0 \tag{1}$$

$$\rho v \frac{du}{dy} = -\frac{d\bar{p}}{dx} + \mu \frac{d^2u}{dy^2} - \rho_p N(u - u_p) - \rho g \tag{2}$$

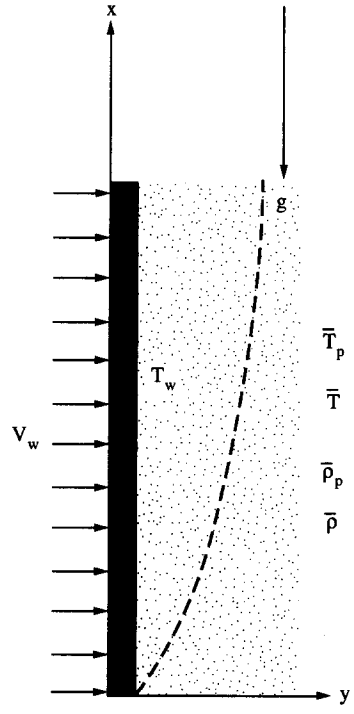

Fig. 1. Flow model and cordinate system.

$$\rho v \frac{dT}{dy} = k \frac{d^2T}{dy^2} + \rho_p c_p N_T (T_p - T) \tag{3}$$

for the fluid phase and

$$\frac{d(\rho_p v_p)}{dy} = 0 \tag{4}$$

$$\rho_p v_p \frac{du_p}{dy} = \nu_p \frac{d}{dy}\left(\rho_p \frac{du_p}{dy}\right) + \rho_p N(u - u_p) - \rho_p g \tag{5}$$

$$\rho_p v_p \frac{du_p}{dy} = 2\nu_p \frac{d}{dy}\left(\rho_p \frac{dv_p}{dy}\right) + \rho_p N(v - v_p) \tag{6}$$

$$\rho_p c_p v_p \frac{dT_p}{dy} = -\rho_p c_p N_T (T_p - T) \tag{7}$$

for the particle phase. It should be mentioned that, in the above equations, the terms containing the momentum transfer coefficient N represent the interphase drag between the phases while the terms containing the heat transfer coefficient N_T represent the interphase heat transfer between the fluid and the particle phases.

The physical boundary conditions for this problem are

$$u(0) = 0 \tag{8a}$$

$$v(0) = -V_w \tag{8b}$$

$$T(0) = T_w \tag{8c}$$

$$u_p(0) = u_{p0} \tag{8d}$$

$$u_p(0) = s \frac{du_p}{dy}(0) \tag{8e}$$

$$v_p(0) = -V_{pw} \tag{8f}$$

$$u(\infty) = 0 \tag{8g}$$

$$T_p(\infty) = T(\infty) \tag{8h}$$

$$\rho_p(\infty) = \bar{\rho}_p \tag{8i}$$

Equations (8a) and (8b) indicate no slip condition and uniform suction or injection for the fluid phase, respectively. Equation (8c) suggests that the fluid temperature at the wall is the same as that of the plate. Equations (8d) and (8e) are two different proposed wall boundary conditions for the particle phase. It should be mentioned here that the exact form of boundary conditions to be satisfied by the particle phase at a surface are currently unknown. However, there is an experimental evidence that particles tend to slip at a boundary. Equation (8e) is borrowed from rarefied gas dynamics to represent this phenomenon since the motion of the particle phase may resemble that of a rarefied gas. Equation (8f) allows for uniform particle-phase wall suction of injection. Equations (8g)–(8i) are ambient conditions for the fluid velocity and the particle-phase temperature and density, respectively.

Additional conclusions and ambient conditions for the particle phase can be obtained by evaluating equations (1)–(7) at $y = \infty$ to yield

$$\frac{d\bar{p}}{dx} = -\bar{\rho} g + \bar{\rho}_p N \bar{u}_p \tag{9a}$$

$$\bar{u}_p = -\frac{g}{N} \tag{9b}$$

$$\bar{T}_p = \bar{T} \tag{9c}$$

$$\bar{v}_p = \bar{v} \tag{9d}$$

where a bar indicates a condition at $y = \infty$.

Substituting equations (9a) and (9b) into equation (2) with

$$\rho = \bar{\rho}[1 + \beta^*(T - \bar{T})] \tag{10}$$

and rearranging gives

$$\bar{\rho} v \frac{du}{dy} = \bar{\rho} g \beta^*(T - \bar{T}) + \bar{\rho}_p g + \mu \frac{d^2u}{dy^2} - \rho_p N(u - u_p) \tag{11}$$

Therefore, Equation (1)–(7) with equation (2) replaced by equation (11) constitute the governing equations for this problem. It should be mentioned that these equations represent a generalization of the dusty-gas equations discussed by Marble [7] to include particle-phase viscosity and buoyancy effects.

It is convenient to nondimensionalize the equations by using

$$y = \frac{YL}{\mathrm{Gr}^{1/4}}, u = \frac{\nu}{L}\mathrm{Gr}^{1/2}U, u_p = \frac{\nu}{L}\mathrm{Gr}^{1/2}U_p, v = \frac{\nu}{L}\mathrm{Gr}^{1/4}V,$$

$$v_p = \frac{\nu}{L}\mathrm{Gr}^{1/4}V_p, T = \bar{T} + (T_w - \bar{T})\theta, T_p = \bar{T}_p + (T_w - \bar{T})\theta_p, \rho_p = \bar{\rho}_p, \mathrm{Gr} = \frac{g\beta^*(T_w - \bar{T})L^3}{\nu^2}$$

$$\kappa = \frac{\bar{\rho}_p}{\rho}, \alpha \frac{NL^2}{\nu \mathrm{Gr}^{1/2}}, H = \frac{L^3 g}{\nu^2 \mathrm{Gr}}, \gamma = \frac{c_p}{c}, \varepsilon = \frac{N_T L^2}{\nu \mathrm{Gr}^{1/2}}, \mathrm{Pr} = \frac{\mu c}{k}, \beta = \frac{\nu_p}{\nu} \tag{12}$$

Upon substituting equation (12) into the governing equations and boundary conditions, the resulting dimensionless equations and conditions become

$$\frac{dV}{dY} = 0 \tag{13}$$

$$\frac{d^2U}{dY^2} - V\frac{dU}{dY} - \kappa\alpha(U - U_p) + \theta + \kappa H = 0 \tag{14}$$

$$\frac{d^2\theta}{dY^2} - \mathrm{Pr}V\frac{d\theta}{dy} + \kappa\gamma\mathrm{Pr}\varepsilon(\theta_p - \theta) = 0 \tag{15}$$

$$\frac{dV_p}{dY} = 0 \tag{16}$$

$$\beta\frac{d^2U_p}{dY^2} - V_p\frac{dU_p}{dY} + \alpha(U - U_p) - H = 0 \tag{17}$$

$$2\beta\frac{d^2V_p}{dY^2} - V_p\frac{dV_p}{dY} + \alpha(V - V_p) = 0 \tag{18}$$

$$V_p\frac{d\theta_p}{dY} + \varepsilon(\theta_p - \theta) = 0 \tag{19}$$

$$U(0) = 0 \tag{20a}$$

$$V(0) = -r_v \tag{20b}$$

$$\theta(0) = 1 \tag{20c}$$

$$U_p(0) = U_{p0} \tag{20d}$$

$$U_p(0) = \omega \frac{dU_p(0)}{dY} \tag{20e}$$

$$V_p(0) = -r_v \tag{20f}$$

$$U(\infty) = 0 \tag{20g}$$

$$\theta_p(\infty) = \theta(\infty) = 0 \tag{20h}$$

It should be mentioned that two forms of wall boundary conditions for U_p are used in the present work. Equation (20d) allows for constant amount of wall particulate slip while equation (20e) is familiar from rarefied gas dynamics and is employed herein to allow for various particle-phase wall conditions which are not known at present. It is noted that when the slip coefficient ω is formally set to zero, a no-slip condition recovers. However, as $\omega \to \infty$ a perfect slip situation occurs.

Equation (13) can be solved directly for V subject to equation (20b) to give $V = -r_v$. In addition, equations (16) and (18) are satisfied by $V_p = V = -r_v$ for the case of uniform particle-phase density distribution. Combining equation (15) with equations (19) and(14) with equation (17) in terms of θ_p and U_p respectively, gives

$$\frac{d^3\theta_p}{dY^3} + \left(\frac{\Pr r_v^2 - \varepsilon}{r_v}\right)\frac{d^2\theta_p}{dY^2} = \varepsilon \Pr(1 + \kappa\gamma)\frac{d\theta_p}{dY} = 0 \tag{21}$$

$$\beta \frac{d^4U_p}{dY^4} + r_v(1+\beta)\frac{d^3U_p}{dY^3} - \alpha\left(1 - \frac{r_v^2}{\alpha} + \kappa\beta\right)\frac{d^2U_p}{dY^2} - r_v\alpha(1+\kappa)\frac{dU_p}{dY} = \alpha\theta \tag{22}$$

where θ and U are related to θ_p and U_p as follows

$$\theta = -\frac{r_v}{\varepsilon}\frac{d\theta_p}{dY} + \theta_p \tag{23}$$

$$U = \frac{H}{\alpha} - \frac{\beta}{\alpha}\frac{d^2U_p}{dY^2} - \frac{r_v}{\alpha}\frac{dU_p}{dY} + U_p \tag{24}$$

Important physical quantities for this flow and heat transfer situation are the fluid-phase wall shear stress, the particle-phase wall shear stress, and the rate of heat transfer at the surface. These quantities are defined as

$$\tau_f = -\mu\frac{du}{dy}(0),\ \tau_p = -\mu_p\frac{du}{dy}(0),\ q_w = -k\frac{dT}{dy}(0) \tag{25}$$

Therefore, the fluid-phase skin-friction coefficient C_f, the particle-phase skin-friction coefficient C_p, and the Nusselt number Nu can be defined, respectively, as

$$C_f = \frac{\tau_f}{\frac{\rho\nu^2}{L^2}\mathrm{Gr}^{3/4}} = -\frac{dU}{dY}(0), \qquad C_p = \frac{\tau_p}{\frac{\rho\nu^2}{L^2}\mathrm{Gr}^{3/4}} = -\kappa\beta\frac{dU_p}{dY}(0)$$

$$\mathrm{Nu} = \frac{q_w}{\frac{k(T_w - T)}{L}\mathrm{Gr}^{1/4}} = -\frac{d\theta}{dY}(0) \tag{26}$$

2. RESULTS AND DISCUSSION

2.1 *Inviscid particle phase*

In the absence of the particle-phase viscosity ($\beta = 0$), a closed-form solution for the governing equations is possible. In this case, equations (21) and (23) are solved directly for θ_p and θ, respectively, subject to the appropriate boundary conditions equations (20c)–(20h). Then, the solution for θ is substituted into equation (22) with $\beta = 0$. The resulting third-order differential equation is solved subject to the boundary conditions given by equations (20a), (20h) and $U_p(\infty) = -(H/\alpha)$ (the dimensionless form of equation (9b)). Equation (24) with $\beta = 0$ is then solved for U. Without going into detail, it can be shown that these solutions can be written as

$$\theta = e^{m_2 Y} \tag{27}$$

$$\theta_p = \frac{e^{m_2 Y}}{\left(1 - \frac{r_v}{\varepsilon} m_2\right)} \tag{28}$$

$$U = A_2\left(1 - \frac{r_v}{\alpha}\lambda_2\right)e^{\lambda_2 y} + A_4\left(1 - \frac{r_v}{\alpha} m_2\right)e^{m_2 Y} \tag{29}$$

$$U_p = A_2 e^{\lambda_2 Y} + A_4 e^{m_2 Y} - \frac{H}{\alpha} \tag{30}$$

where

$$m_2 = -\frac{1}{2}\left[\left(\frac{\mathrm{Pr} r_v^2 - \varepsilon}{r_v}\right) + \sqrt{\left(\frac{\mathrm{Pr} r_v^2 - \varepsilon}{r_v}\right)^2 + 4\mathrm{Pr}\varepsilon(1 + \kappa\gamma)}\right] < 0 \tag{31}$$

$$\lambda_2 = -\frac{1}{2}\left[\left(\frac{r_v^2 - \alpha}{r_v}\right) + \sqrt{\left(\frac{r_v^2 - \alpha}{r_v}\right)^2 + 4\alpha(1 + \kappa)}\right] < 0 \tag{32}$$

$$A_4 = \frac{\alpha}{r_v m_2\left[m_2^2 + \left(\frac{r_v^2 - \alpha}{r_v}\right)m_2 - \alpha(1 + \kappa)\right]}, A_2 = -A_4\left(\frac{1 - \frac{r_v}{\alpha} m_2}{1 - \frac{r_v}{\alpha}\lambda_2}\right) \tag{33}$$

The fluid-phase skin-friction coefficient C_f and the Nusselt number Nu for this case are given, respectively, by

$$C_f = -\lambda_2 A_2\left(1 - \frac{r_v}{\alpha}\lambda_2\right) - m_2 A_4\left(1 - \frac{r_v}{\alpha} m_2\right), \mathrm{Nu} = -m_2 \tag{34}$$

Numerical evaluations of the flow and thermal solutions given by equations (27)–(34) are performed for various parametric conditions and illustrated graphically in Figs 2–5 and Table 1.

Figures 2 and 3 present typical tangential velocity profiles for both the fluid and the particle phases U and U_p for various values of the particles loading κ, respectively. Increases in the particle loading have a tendency to increase the drag force between the phases causing a slower motion of the fluid. This produces a reduction in the particle-phase tangential velocity as well since the particle phase is being dragged along by the fluid. These facts are clearly illustrated in Figs 2 and 3. It should be noted here that for vanishing and small values of ($\kappa = 0, 0.1$)

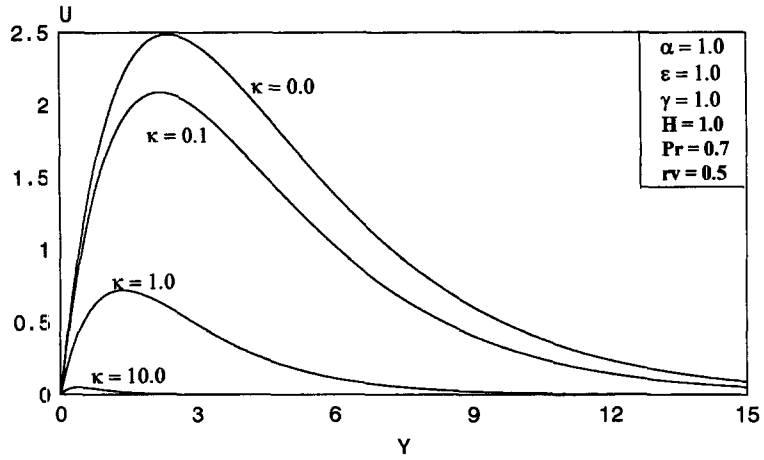

Fig. 2. Variation of fluid velocity profiles with different κ.

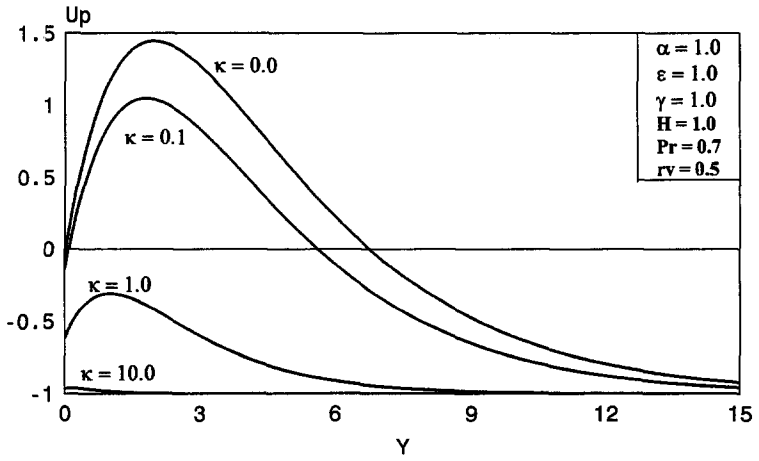

Fig. 3. Variation of particulate velocity profiles with different κ.

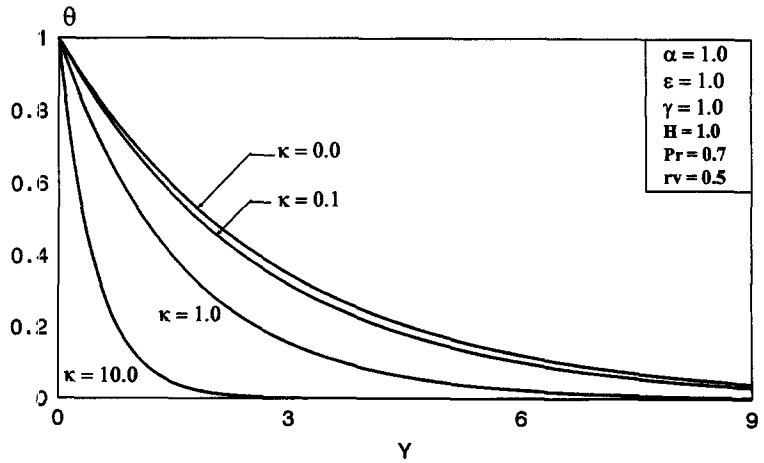

Fig. 4. Variation of fluid temperature profiles with different κ.

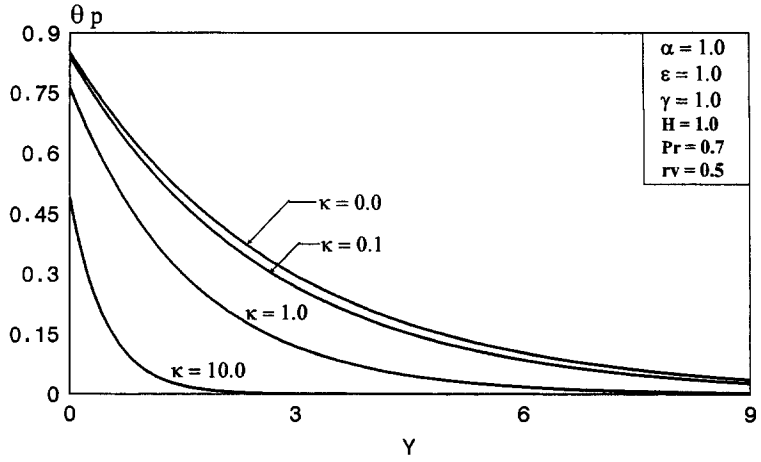

Fig. 5. Variation of particulate temperature profiles with different κ.

U and U_p approach the correct limits (0 and -1, respectively) at large values of Y. However, in Figs 2 and 3, the range of Y was stopped at $Y=15$ to show the changes in the curves better.

Figures 4 and 5 show representative temperature profiles for both the fluid and the particle phases θ and θ_p at different particle loading levels, respectively. It is observed in these figures that both θ and θ_p decrease as κ increases. This is obvious since more fluid-phase energy will be transferred to more particles but the individual particles will receive less energy from the fluid phase as κ increases.

2.2 *Viscous uniform particle phase*

For a viscous particle phase ($\beta \neq 0$) and by neglect of the particle-phase viscous dissipation, the energy equations for both the fluid and particle phases remain the same as those of the inviscid particle-phase case. Therefore, the solutions for θ and θ_p given by equations (27) and (28) still hold for $\beta \neq 0$. However, the momentum equations for the particle phase will be different. For this case, the solutions $V_p = V = -r_v$ still satisfy equations (16) and (18), and equations (22) and (24) are solved for U_p and U, respectively, subject to equations (20a)–(20h). It can be shown

$$U = B_2 F e^{n_2 Y} + B_3 S e^{n_3 Y} + B_5 Z e^{m_2 Y} \tag{35}$$

$$U_p = B_2 e^{n_2 Y} + B_3 e^{n_3 Y} + B_5 e^{m_2 Y} - \frac{H}{\alpha} \tag{36}$$

where

$$F = 1 - \frac{\beta}{\alpha} n_2^2 - \frac{r_v}{\alpha} n_2, S = 1 - \frac{\beta}{\alpha} n_3^2 - \frac{r_v}{\alpha} n_3, Z = \frac{\beta}{\alpha} m_2^2 + \frac{r_v}{\alpha} m_2 - 1 \tag{37}$$

Table 1. Representive values for C_f, C_p and Nu, reference values: $\alpha = 1$, $\beta = 0.5$, $\kappa = 1$, $\omega = 1$, $H = 1$, $r_v = 0.5$

	C_f	C_p	Nu
Reference	1.46272	−0.17157	0.61743
$\alpha = 0.1$	1.76814	−2.57427	0.61743
$\beta = 0$	1.40715	0	0.61743
$\kappa = 0$	2.85714	0	0.35000
$\omega = 0$	1.60718	−0.48759	0.61743
$H = 0.1$	1.32940	0.19009	0.61743
$r_v = 0.1$	6.22223	0.72523	0.13904

$$B_5 = \frac{\alpha}{\beta m_2\left[m_2^3 + \frac{r_v}{\beta}(1+\beta)m_2^2 - \frac{\alpha}{\beta}\left(1 - \frac{r_v^2}{\alpha} + \kappa\beta\right)m_2 - \frac{r_v\alpha}{\beta}(1+\kappa)\right]} \tag{38}$$

where m_2 is the same as given by equation (31) for $\beta = 0$ and n_2 and n_3 are the two negative roots of the cubic equation

$$n^3 + \frac{r_v}{\beta}(1+\beta)n^2 - \frac{\alpha}{\beta}\left(1 - \frac{r_v^2}{\alpha} + \kappa\beta\right)n - \frac{r_v\alpha}{\beta}(1+\kappa) = 0 \tag{39}$$

The constants B_2 and B_3 will be different depending on the particle-phase velocity boundary condition employed at the wall. It can be shown that for $U_p(0) = U_{p0}$, B_2 and B_3 take on the forms

$$B_2 = \frac{B_5 Z + S\left(B_5 - U_{p0} - \frac{H}{\alpha}\right)}{F - S}, B_3 = \frac{B_5 Z + F\left(B_5 - U_{p0} - \frac{H}{\alpha}\right)}{S - F} \tag{40}$$

and for $U_p(0) = \omega \dfrac{dU_p(0)}{dY}$

$$B_2 = \frac{OZB_5 - S\left(PB_5 + \frac{H}{\alpha}\right)}{OF - SN}, B_3 = \frac{NZB_5 - F\left(PB_5 + \frac{H}{\alpha}\right)}{NS - OF} \tag{41}$$

where

$$N = 1 - \omega n_2, O = 1 - \omega n_3, P = \omega m_2 - 1 \tag{42}$$

The appropriate solutions for C_f, C_p and Nu for this particular case ($\beta \neq 0$) can be shown to be

$$C_f = -n_2B_2F - n_3B_3S - m_2B_5Z, C_p = -\kappa\beta(n_2B_2 + n_3B_3 + m_2B_5), \mathrm{Nu} = -m_2 \tag{43}$$

It should be mentioned that if β is equated to zero in equations (35)–(43), the inviscid particle-phase solutions reported earlier are recovered.

Figures 6 and 7 depict the effect of the ratio of the particle-to-fluid-phase viscosity β on the tangential velocity profiles of both phases. These figures are based on the fixed particle-phase boundary condition $U_p(0) = U_p = 0.5$. Increases in the viscosity ratio β have the tendency

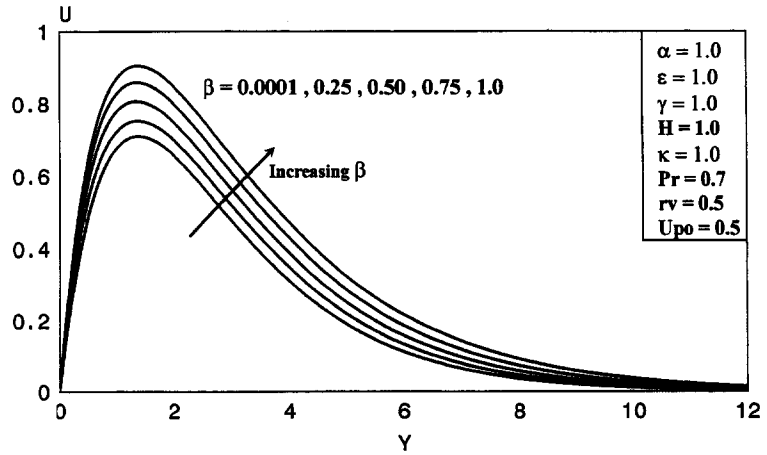

Fig. 6. Variation of fluid velocity profiles with different β.

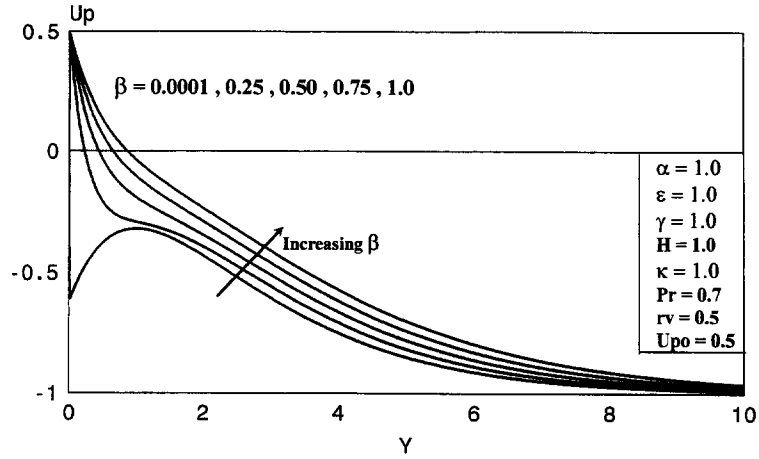

Fig. 7. Variation of particulate velocity profiles with different β.

to increase the magnitudes of the fluid- and particle-phase inertia effects in comparison with the buoyancy effect. This has the effect of increasing the tangential velocities of both phases as clearly depicted in Figs 6 and 7.

Figures 8–10 illustrate the influence of the slip coefficient ω on the tangential velocity and temperature profiles of both the fluid and the particle phases, respectively. In general, as the

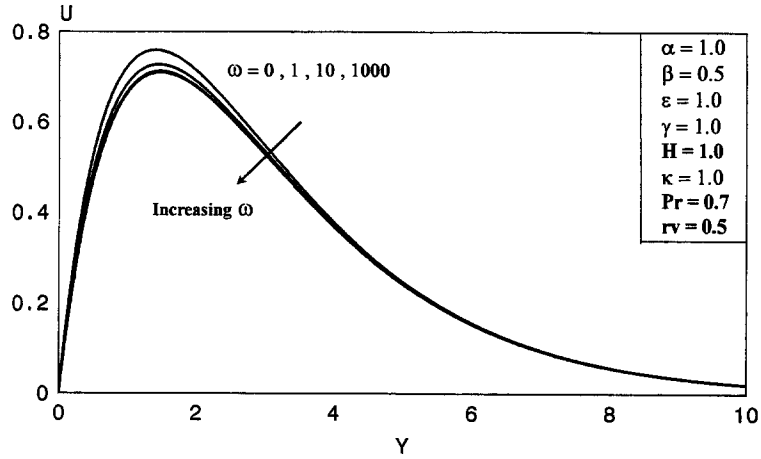

Fig. 8. Variation of fluid velocity profiles with different ω.

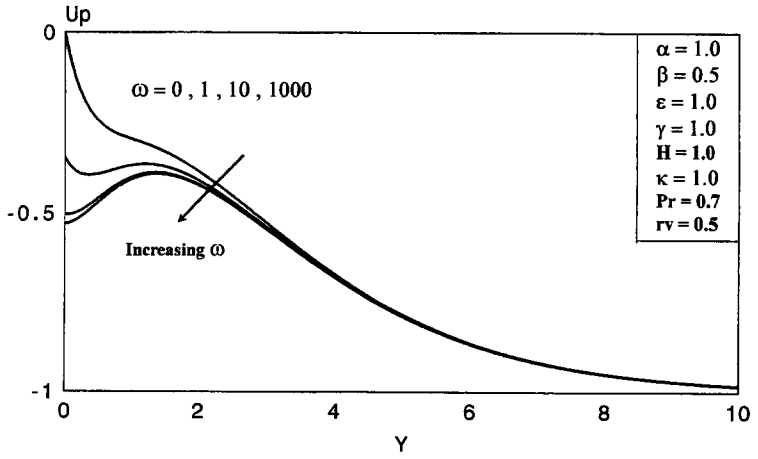

Fig. 9. Variation of particulate velocity profiles with different ω.

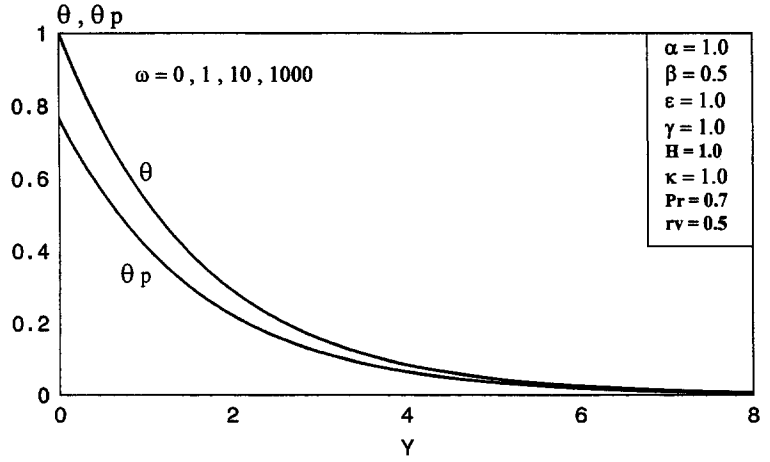

Fig. 10. Variation of temperature profiles with different ω.

particle-phase wall slip increases, it becomes harder for the carrier fluid to move it. Thus, causing the fluid-phase tangential velocity to decrease. As a result, the particle-phase tangential velocity decreases. In addition, the slip coefficient ω seems to have no effect on both θ and θ_p as clearly seen from Fig. 10.

Table 1 illustrates the effects of the parameters α, β, κ, ω, H, r_v on the values of the fluid-phase skin-friction coefficient C_f, the particle-phase skin-friction coefficient C_p, and the Nusselt number Nu. It is clearly observed from this table that C_f increases as either β or H increases and decreases as either of r_v increases. Also, increases in the values of r_v or H cause reductions in the values of C_p. As expected, the Nusselt number is increased only by increasing either r_v or κ.

3. CONCLUSION

A mathematical model for free-convection of a two-phase fluid–particle suspension is formulated and applied to the problem of flow and heat transfer over an infinite porous vertical plate. The model accounts for particulate viscous effects and for finite particulate volume fraction. Analytical solutions for the velocity and temperature profiles of both phases as well as their skin-friction coefficients and the Nusselt number for the fluid phase for the cases of inviscid and viscous particle phase are developed. Typical graphical results illustrating the influence of various physical parameters on the behavior of both phases are presented and discussed. It is found that increases in either of the particle loading or the wall suction caused reductions in the velocities of both phases as well as the skin-friction coefficient for the fluid phase and increases in the Nusselt number. In addition, as the wall particulate slip was increased, the velocities of both phases and the fluid-phase skin-friction were also decreased while the Nusselt number remained constant. It should be mentioned that no comparisons with experimental data were performed as these data appear to be lacking at present. It is hoped that the exact solutions reported herein will serve as a stimulus for experimental work and as a vehicle for understanding natural convection for a particulate suspension and for investigating alternate particle-phase stress models.

REFERENCES

1. Gebhart, B., Jaluria, Y., Mahajan, R. L., and Sammakia, B., *Buoyancy-Induced Flows and Transport*, Hemisphere, New York, 1988, p. 914.
2. Kierkus, W. T. An Analysis of Laminar Free Convection Flow and Heat Transfer about an Inclined Isothermal Flat Plates. *Int. J. Heat and Mass Transfer*, 1968, **11**, 241–253.

3. Hassan, K. and Mohamed, S. Natural Convection from Isothermal Flat Surfaces. *Int. J. Heat and Mass Transfer,* 1970, **13,** 1873–1886.
4. Sparrow, E. M. and Gregg, J. L. Laminar Free Convection from a Vertical Plate with Uniform Surface Heat Flux. *Trans. ASME,* 1956, **78,** 435
5. Elsayed, M. M., and Fathalah, K. A., *Temperature Distribution in a Direct Solar Heater*, 72nd annual meeting of AIChE, Paper No. P-7d, 1979.
6. Fathalah, K. A. and Elsayed, M. M. Natural Convection Due to Solar Radiation Over a Non-Absorbing Plate With and Without Heat Losses. *Int. J. Heat & Fluid Flow,* 1980, **2,** 41–45.
7. Marble, F. E. Dynamics of Dusty Gases. *Annual Review of Fluid Mechanics,* 1970, **2,** 297–446.
8. Ishii, M., *Thermo-Fluid Dynamic Theory of Two-Phase Flow*, Eyrolles, Paris, 1975.
9. Berlemont, A. *et al.* Particle Lagrangian Simulation in Turbulent Flows. *International Journal of Multiphase Flow,* 1990, **16,** 19–34.
10. Gadiraju, M., Peddieson, J. and Munukutla, S. Exact Solutions for Two-Phase Vertical Pipe Flow. *Mechanics Research Communications,* 1992, **19,** 7–13.
11. Gidaspow, D. Hydrodynamics of Fluidization and Heat Transfer: Super Computer Modeling. *Applied Mechanics Reviews,* 1986, **39,** 1–23.
12. Tsuo, Y. P. and Gidaspow, D. Computation of Flow Patterns in Circulating Fluidized Beds. *AIChE Journal,* 1990, **36,** 888–896.
13. Drew, D. A. Mathematical Modelling of Two-Phase Flow. *Annual Review of Fluid Mechanics,* 1983, **15,** 261–291.
14. Drew, D. A. and Segal, L. A. Analysis of Fluidized Beds and Foams using Averaged Equations. *Studies in Applied Mathematics,* 1971, **50,** 233–252.

(Received 27 November 1996; accepted 18 April 1997)

APPENDIX

NOMENCLATURE

C	Skin-friction coefficient ($\tau L^2/\rho\nu\ \mathrm{Gr}^{3/4}$))
c	Fluid-phase specific heat at constant pressure
d	Particle diameter
g	Gravitational acceleration
Gr	Fluid-phase Grashof number ($g\beta \times (T_w - \bar{T})L^3/\nu^2$)
H	Buoyancy parameter ($L^3 g/\nu^2 \mathrm{Gr}$))
k	Fluid-phase thermal conductivity
L	Characteristic length
N	Momentum transfer coefficient ($18\mu/(\rho_g d^2)$)
N_T	Heat transfer coefficient ($12k(\rho_g d^2 c_p)$)
Nu	Nusselt number ($q_w L/(k(T_w - \bar{T})\mathrm{Gr}^{1/4})$)
p	Fluid-phase pressure
Pr	Fluid-phase Prandtl number ($\mu c/k$)
q_w	Dimensional heat transfer rate
r_v	Wall suction parameter ($V_w L//\nu\mathrm{Gr}^{1/4}$))
s	Particle-phase dimensional slip coefficient
T	Fluid-phase dimensional temperature
u	Fluid-phase dimensional axial or tangential velocity
U	Fluid-phase dimensionless tangential velocity ($uL/\nu\mathrm{Gr}^{1/2}$))
v	Fluid-phase dimensional normal velocity
V	Fluid-phase dimensionless normal velocity ($VL/\nu\mathrm{Gr}^{1/4}$))
x	Dimensional axial or tangential distance
y	Dimensional normal distance
Y	Dimensionless normal distance ($y\mathrm{Gr}^{1/4}/L$)

Greek symbols

α	Momentum inverse Stokes number ($NL^2/\nu\mathrm{Gr}^{1/2}$))
β	Viscosity ratio (ν_p/ν)
β^*	Thermal expansion coefficient
ε	Temperature inverse Stokes number ($N_T L^2/(\nu\mathrm{Gr}^{1/2})$)
γ	Ratio of specific heats (c_p/c)
κ	Particle loading ($\bar{\rho}_p/\rho$)
μ	Fluid-phase dynamic viscosity
ν	Fluid-phase kinematic viscosity (μ/ρ)
ω	Particle-phase dimensionless wall slip coefficient ($s\mathrm{Gr}^{1/4}/L$)
ρ	Fluid-phase density
ρ_g	Density of particulate material
τ	Dimensional shear stress
θ	Fluid-phase dimensionless temperature ($(T - \bar{T})/(T_w - \bar{T})$)

Subscripts

0, w	At the wall
f	Fluid phase
p	Particle phase

Superscripts

–	Value at infinity or ambient value